Original citation:
Kellner, Quirin, Worwood , D, Widanage, D. W. and Marco, James (2017) Electrical and thermal behaviour of pouch-format lithium ion battery cells under high-performance and standard automotive duty-cycles. In: IEEE Vehicle Power and Propulsion Conference, Belfort, France, 11-14 Dec 2017. Published in: IEEE Vehicle Power and Propulsion Conference (In Press)

Permanent WRAP URL:
http://wrap.warwick.ac.uk/95986

Thermal analysis of fin cooling large format automotive lithium-ion pouch cells

Daniel Worwood, Quirin Kellner, Elham, Hosseinzadeh, David Greenwood, James Marco
WMG
University of Warwick
Coventry, United Kingdom
e-mail: d.worwood@warwick.ac.uk

David Mullen
Ryan McGlen
Kevin Lynn
Aavid Thermacore Europe
Ashington, United Kingdom
e-mail: David.Mullen@aavid.com
e-mail: Ryan.McGlen@aavid.com
e-mail: Kevin.Lynn@aavid.com

***Abstract*—Conductively cooling the surface of lithium-ion pouch cells may simplify the external cooling mechanism, as heat transfer mediums are not routed across the cell surface. In this paper, the thermal performance of cooling cells with metallic fins is analysed using a developed test rig and thermal model. Results indicate that single edge fin cooling with aluminum sheets is effective in limiting surface temperature gradients to below circa 5℃ for cells subject to realistic EV and mild PHEV duty cycles. For aggressive track racing EV cycles, double edge fin cooling is required to limit surface temperature gradients to below 12℃ .**

Keywords—Lithium-ion battery, battery thermal management, fin cooling, EV, PHEV

I. INTRODUCTION

Full electric (EV), hybrid electric (HEV) and plug-in hybrid electric (PHEV) vehicles are witnessing increased market penetration rates [1] due to advances in battery technology that enable their adoption for a lower cost than previously possible [2]. However, battery requirements which enable electrified vehicles to challenge and further increase their competitiveness against conventional internal combustion engine (ICE) vehicles - such as increased energy and power density [3] - necessitate greater consideration to the design of the battery thermal management system (BTMS). This system must ensure that the thermals of the individual battery cells – contained within battery modules and full packs - are adequately controlled, such as to minimise detrimental thermal related effects on battery performance [4], durability [5] and avoid thermal runaway events [6], [7]. Specifically, the optimum lithium-ion battery operating temperature has been reported by many researchers to lie within a range of 15-35 ℃ [8], however, other accounts [9] suggest this range should be constrained to 25±5 ℃ to further limit the rate of parasitic side reactions occurring within the cell that increases the rate of capacity fade as the temperature increases [10].

In addition to the need for absolute control over the volume averaged battery cell operating temperature ($T_{vol,cell}$), it is imperative that temperature gradients occurring through the internals of individual cells and between cells contained within battery modules and packs be minimised by the BTMS [11]. These temperature gradients are known to accelerate ageing through the loss of cyclable lithium [12], [13], prompting many [11], [14]–[16] to suggest an upper tolerable limit of 5□ for temperature gradients through and between cells. Effective BTMS's must therefore be designed in such a manner as to ensure that the method of absolute temperature control does not induce an unfavorable temperature gradient that can compromise the benefit of maintaining the cell within its optimum temperature range.

Numerous approaches to battery thermal management have been investigated [8]. Common approaches include actively passing air over the battery surface [15], [17], attaching indirect liquid cooling plates onto the battery surface [18], [19], passing dielectric oil directly across the battery surface [20] and attaching metallic cooling fins onto the surface to conduct heat away from the battery to a surface cooled elsewhere (i.e. fin cooling) [21]. Other emerging techniques for battery thermal management include attaching [14] or inserting [22], [23] heat pipes onto/into the battery to further reduce the thermal resistance of conventional air and liquid cooling approaches for improved thermal control. Phase change material cooling is another method that has received growing attention [24], [25]. The plethora of options for battery thermal management exists due to inherent trade-offs between balancing the required thermal control with other conflicting yet desirable characteristics of the BTMS design, which includes low cost, weight and volume requirements [26].

Although liquid cooled designs may show exemplary thermal control and efficiency relative to those using air, the risk of leakage within battery packs is of great concern given the severity of a cell short circuit event and thermal runaway [8]. Relative to indirect liquid plates attached to the battery surface, battery packs employing fin cooling have the benefit of dramatically reducing the number of manifold connections required (and hence the leakage risk) given that heat is conducted to a side or base cold plate that may require only one inlet and outlet. Fin cooled designs may therefore be less costly and less maintenance intensive than other indirect liquid cooling options such as in [27] that require more complex piping arrangements [28].

Previous research [29] suggests that single edge aluminum fin cooling - with a practical sandwich fin thickness <1.5 mm - of large format (≥40 Ah) pouch type batteries is unsuitable under a sustained C-rate of 3C, due to the development of large maximum cell temperature gradients ($\Delta T_{max,cell}$) of 22.9□. However, such a heat generation condition may not be a representative design point for the thermal management system in commercial EVs and PHEVs, as the transient C-rate profile is highly dynamic with a lower overall time averaged C-rate under realistic usage conditions [30].

In this paper, a comprehensive thermal analysis on the thermal performance of fin cooling for large format pouch cells subject to duty cycles representative of an EV, PHEV and performance EV is conducted. The paper is structured as follows. Section II outlines the design of the test rig used to experimentally measure the thermal performance of pouch cells subject to fin cooling. Section III discusses the battery thermal model used to enable an extended simulation analysis into fin cooling, whereby Section IV includes the duty cycle profiles used. Experimental results from the test rig tracking the temperature evolution are contained in Section V, which is also compared to the simulation results from the thermal model testing its accuracy. In Section VI, an extended simulation analysis is conducted to investigate the thermal performance of two edge fin cooling (with both copper and aluminum materials) as a thermal solution for pouch cells under aggressive EV racing conditions. Further work and conclusions are contained within Section VII and Section VIII respectively.

II. TEST RIG

The test rig design consists of contacting 0.5 mm thick fins onto both the front and back surface of large format 53 Ah pouch cells with a graphite anode and NMC cathode. One edge of the fins is bent with a bend radius of 1 mm to form 25 mm of flat contact length. The contact length of the fin is clamped under pressure onto an indirect liquid cooled cold plate to dissipate the heat that is conducted through the fin from the cell surface. A water-glycol mixture is pumped through the cold plate at a regulated set-point temperature of 25 ℃ with a flowrate of 10 L.min^{-1}. The test rig is capable of cycling three cells at once, with a total of 6 cooling fins. The cells are thermally isolated from one another vie the use of polystyrene and rigid FOAMGLASS® slabs. The FOAMGLASS® is incompressible and enables uniform pressure to be applied via the clamps along the length of the cooling fin edge onto the cold plate. Pressure onto the stack to ensure good contact of cooling fins onto the battery surface is achieved via the use of a hand operated air wedge bag. The experimental set up can be viewed in Figure 1. Given the insulation present on the back of the fin together with symmetry planes present, the cooling arrangement with the 0.5 mm thick fins is set up to emulate that of a 1 mm thick fin when

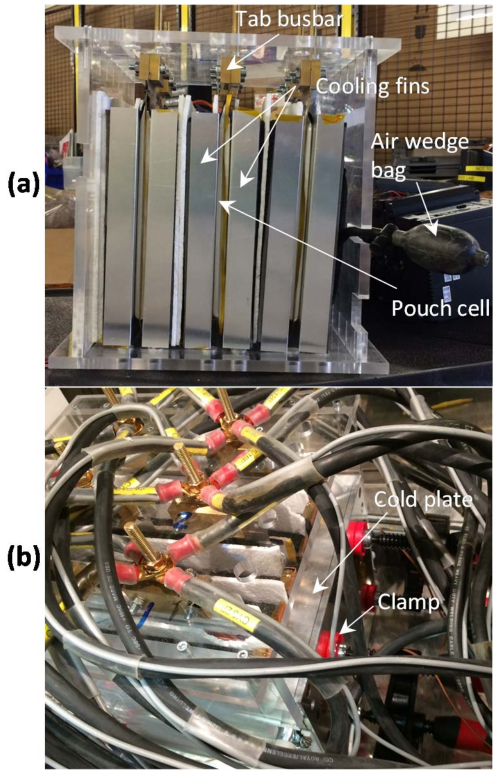

Figure 1: Experimental set-up of test rig (a) front view with aluminum fins (b) close up of copper fin contact onto cold plate

sandwiched directly between adjacent cells i.e. symmetrical stack cooling.

Buffer foam is placed in between the fin contact length and FOAMGLASS ® to enable placement of thermocouples along the length of the fin contact. Insulating wool is placed within the top of the test rig to minimise the effect of external ambient cooling (not shown in Figure 1). The dimensions of the cooling fins and thermal properties used for the subsequent thermal model are displayed in Table 1.

Table 1: Dimensions and thermal properties of fins used

Fin material	Fin body dimensions		
	Height [mm]	*Length [mm]*	*Thickness [mm]*
Copper	220	235	0.5
Aluminium	220[a]	235[a]	0.5
Fin material	**Fin thermal properties at 25℃**		
	Thermal conductivity [W.m^{-1}.K^{-1}]	*Density [kg.m^{-3}]*	*Heat capacity [J.kg^{-1}.K^{-1}]*
Copper	385	8960	385
Aluminium	220	2700	900

The temperature evolution of the fin surface is tracked via the use of 15 T-type thermocouples. The placement of thermocouples across the fins is shown in Figure 2. The hottest point on the fin body is represented by location 5 (which is furthest from the external cooling plate) and the coolest point by location 9 (closest to external cold plate).

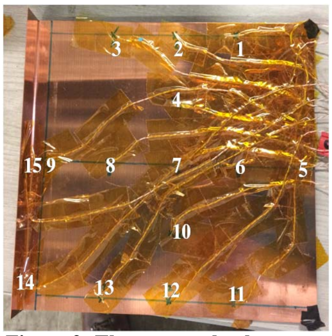

Figure 2: Thermocouple placement

III. Battery Thermal Model

A schematic of the 3-D battery fin cooled model (using COMSOL) is displayed in Figure 3. The modelling approach adopted for the bulk battery material and tabs has been used previously and is described in [29], [31]. This approach includes specifying heat sources within both the bulk cell body and positive and negative tabs. Here, half a cell geometry is used to utilise the symmetry planes present.

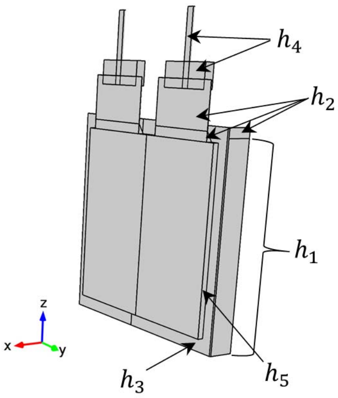

Figure 3: Schematic of the battery cell thermal model with single edge fin cooling

Heat transfer coefficients are specified on the cell and fin boundaries denoted by the h coefficients [W.m^{-2}.K^{-1}]. Here, h_1 is the heat transfer coefficient along the clamped fin edge onto the cold plate, h_2 from the top of the fin edge and the exposed tab body, h_4 from the tab busbar blocks and protruding screw, h_3 from the exposed edges of the fin and on the front of the fin to account for non-ideal insulation and h_5 from the edges of the cell.

The battery heat generation within the cell body, which is assumed uniform throughout the cell material, is calculated through use of a 1-D electrochemical model described in [31]. Joule heating in the tabs is described via:

$$q_t''' = \frac{I^2 R_t}{v_t} \tag{1}$$

Where q_t''' is the volumetric tab heat generation rate [W.m^{-3}], I the cell current [A], R_t the tab resistance [Ω] and v_t the volume of the bulk tab material [m^3]. The resistance for the copper tab and aluminum tab is calculated from the expression for resistivity, with a value of 3.36x10^{-5} Ω and 5.30x10^{-5} Ω for each tab respectively. Values for the cell body dimensions and thermal properties used in the thermal modelling are displayed in Table 2.

Table 2: Dimensions and thermal properties of the cell used in the thermal analysis

Cell body dimensions		
Height [mm]	***Length [mm]***	***Thickness [mm]***
190	208	11.8
Cell body bulk thermal properties		
Thermal conductivity [W.m^{-1}.K^{-1}]	***Density [kg.m^{-3}]***	***Heat capacity [J.kg^{-1}.K^{-1}]***
x = 0.28, y=z= 30	2390	1500

IV. Duty Cycles

The thermal performance of the cells under fin cooling is analysed subject to an EV, PHEV and performance EV duty cycle. The PHEV and performance EV cycles are viewable in Figure 4. It is out the scope of this paper to discuss the derivation of the duty cycles, however, details of both can be viewed in [30] for the PHEV cycle (which reflects a 16 kWh medium sized vehicle subject to 3 loops of the WLTP Class 3 cycle using 82 53 Ah cells) and [31] for a similar performance EV cycle. For the EV case, a 1C discharge condition is analysed. The starting state of charge (SOC) for the cells during all cycles is 100%, with the exception of the performance EV cycle where the initial SOC of the cells is at 95% SOC.

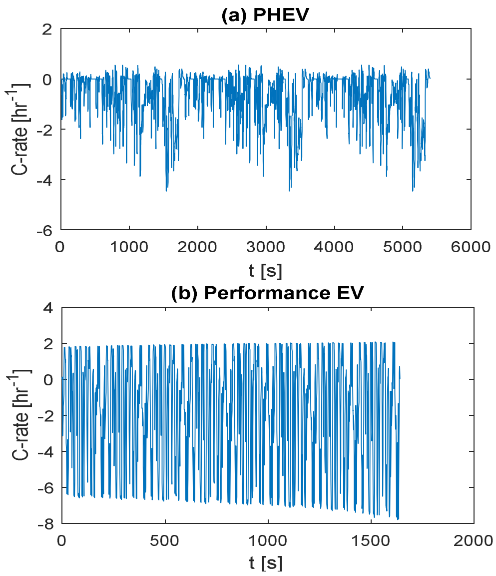

Figure 4: Duty cycles for (a) PHEV (b) performance EV

V. Test Rig Results and Battery Thermal Model Validation

The accuracy of the developed battery thermal model is compared against experimental test data acquired from the test rig during the analysed duty cycles. For the experimental results, the average temperature measurements across all the cell samples are taken (6 cells in total). The h value parameters used as input into the thermal model, with respect to Figure 3, are displayed in Table 3.

Table 3: Heat transfer coefficient values used in the thermal model

	h $[W.m^{-2}.K^{-1}]$				
	h_1	h_2	h_3	h_4	h_5
Value $[W.m^{-2}.K^{-1}]$	750	10	1.1	25	20

Values for h_1 are within the range achievable from liquid cooling using water-glycol [32], whereby the value of h_4 describes convection at the busbars which is exposed to the air circulation within the climate chamber ambient [33]. Natural convection with air is specified at the fin portion of the tab which is protected from the climate chamber air circulation effect by the test rig roof. A value of 20 $W.m^{-2}.K^{-1}$ is specified on the edges of the pouch cell to account for the edge effects [34]. A small value for h_3 is chosen to account for non-perfect thermal isolation on the exposed surfaces of the fin.

The results for both the maximum fin temperature (T_{max}) at location 5 in Figure 2, and maximum fin temperature gradient (ΔT_{max}) from the difference between thermocouple measurements at locations 5 and 9 for all duty cycles are shown in Figure 5. As good thermal contact is achieved between the fin and cell surface given the stack pressure applied via the air wedge bag, and that the metallic fin material is thin (0.5mm), temperature readings on the surface of the fin are assumed to represent the cell surface temperature due to the negligible thermal resistance. This assumption is justifiable given that readings from an additional thermocouple placed on the edge of the cell body under the fin near location 5 provided negligible deviation (<1%) from the fin temperature reading at location 5.

At the end of the performance EV cycle, Figure 5 (a) highlights that the maximum experimental fin temperature reaches 52.7 °C for the aluminum fin and 49.5 °C for the copper fin. These are unacceptable values given that it far exceeds the optimal operating range of lithium-ion cells (circa 25-35 °C). In addition, the aggressiveness of the duty cycle results in a large temperature gradient across the fin and cell surface as seen in Figure 5 (b). Here, the peak experimental ΔT_{max} reaches 18.2 °C and 16.4 °C for the aluminum and copper fin respectively, leading to unfavorable thermal conditions for the cell. The final SOC value for the cells following completion of the performance EV cycle using coulomb counting is 11.6%.

For the 1C EV discharge case, aluminum fins can limit T_{max} to below 35.0 °C, with a peak value for ΔT_{max} of 6.4°C. Provided the cell is not discharged into the deep discharge region below 10% SOC, ΔT_{max} can remain below 5 °C.

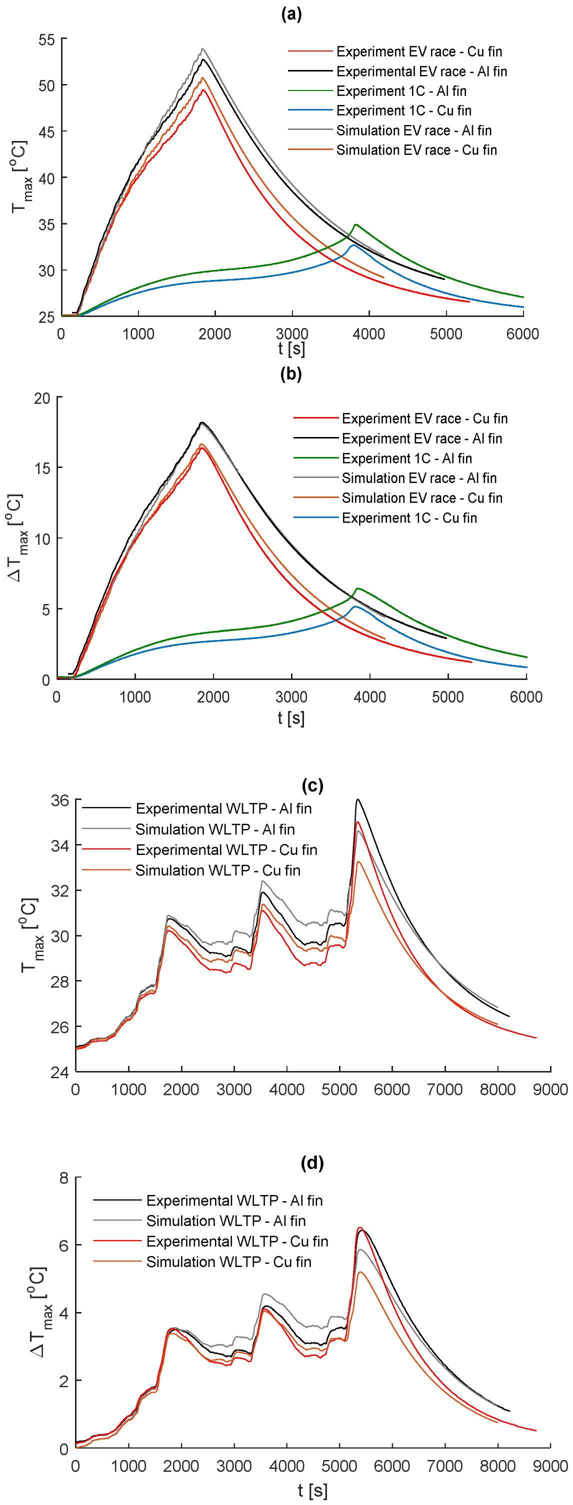

Figure 5: Experimental and simulation results for (a) T_{max} for EV duty cycles (b) ΔT_{max} for EV duty cycles (b) T_{max} for PHEV duty cycle (c) ΔT_{max} for PHEV duty cycle

For the PHEV duty cycle, as seen in Figure 5 (c), the experimental T_{max} value reaches 36.0 °C and 35.0 °C at the end of the third WLTP loop for the aluminum and copper fins respectively, in which the cell SOC is at 4.9%. Similarly, the corresponding ΔT_{max} values reach 6.5 °C for both fins as seen in Figure 5 (d). Provided, the cell SOC is not permitted to drop below 10% (i.e. past 5238s), ΔT_{max} can be limited to below 5 °C for both fin materials.

Overall, Figure 5 highlights that the thermal model provides good agreement to the experimental results for both the EV and PHEV duty cycles for both fin materials. The largest mean absolute percentage error (MAPE) occurs for the performance EV cycle with the copper fin, whereby the MAPE value for the T_{max} estimate is 2.54%. The maximum percentage error occurs for the WLTP cycle with the copper fin in the estimate of T_{max}, with a value of 6.1%.

VI. Extended Simulation Analysis

Given the poor thermal performance of single edge fin cooling under the performance EV cycle, the geometry of the thermal model is extended to include two edge cooling to gauge the level of improvement. A schematic of the two edge cooled fin model is shown in Figure 6. Symmetry planes are included to extend the geometry whereby all input values are as used in the single edge cooled model.

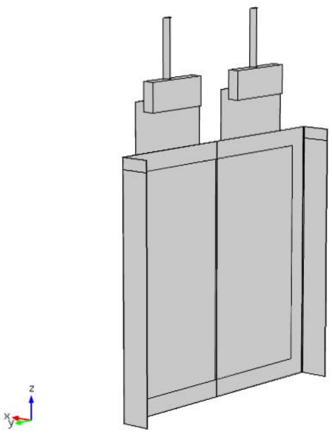

Figure 6: Schematic of battery cell thermal model with two edge fin cooling

The simulation results comparing two edge cooling to single edge cooling under the performance EV cycle are shown in Figure 7. For the aluminum fin, the value for T_{max} reduces from 53.9 °C to 45.8 °C at the end of the cycle upon the adoption of two edge cooling, giving a 15.0% decrease. For the copper fin, T_{max} reduces from 50.7 °C to 41.1 °C, a 18.9% decrease.

From Figure 7 (b) it is also observed that ΔT_{max} is vastly reduced upon the adoption of two edge cooling. For the aluminum fin, ΔT_{max} at the end of the cycle reduces from 18.1 °C with single edge cooling to 11.3 °C with two edge cooling, providing a 37.6% decrease. For the copper fin, ΔT_{max} reduces from 16.7 °C to 8.8 °C, giving a 47.3% decrease. These results imply that two edge fin cooling is particularly effective for fin materials with greater thermal conductivity.

Whilst the copper fin gives an improvement over the aluminum fin, its weight renders it an inappropriate fin choice. The weight metric of the fin system is defined by:

$$Weight\ metric = \frac{Cell\ weight}{Cell\ weight + fin\ weight}$$

Whereby values closer to unity provide a lighter design. Given the fin geometry in Figure 6, the aluminum fin gives a weight metric of 0.86, whereas the copper fin gives a weight metric of 0.65 which is inefficient. Fin cooling with conventional copper and aluminum materials may, therefore, be inappropriate for performance EV applications given the deficiency in thermal performance even when two edge cooling is applied.

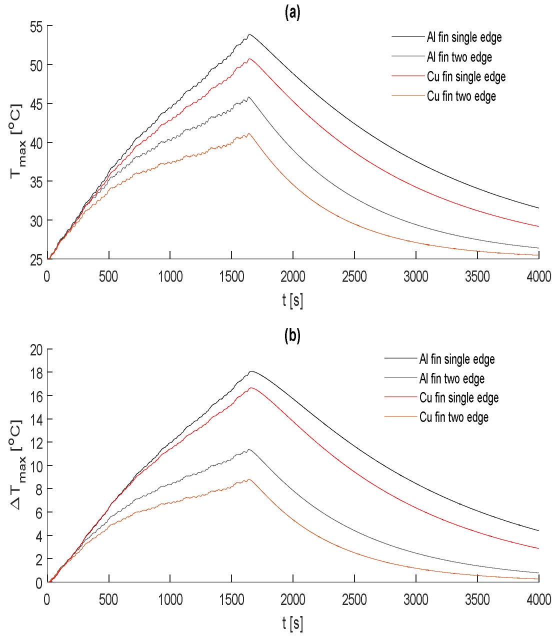

Figure 7: Two edge vs. single edge fin cooling simulation results under the performance EV cycle with (a) T_{max} evolution (b) ΔT_{max} evolution

VII. Further Work

Fin materials with a higher thermal conductivity and much lower density than copper should be investigated to target aggressive performance EV applications, given the need for increased thermal performance over aluminum fins whilst retaining a similar or improved weight metric.

The method of edge cooling must also be altered for practical applications (i.e. remove the 25 mm of flat contact length to enable compact packing of cells). This will require further design study.

VIII. CONCLUSION

Experimental results from the test rig and thermal modelling analysis highlights that single edge fin cooling with aluminum sheets (1 mm total reflective sandwich thickness) is effective in limiting the maximum cell surface temperature gradients ($\Delta T_{max,cell}$) of large format pouch cells to below 5 ℃ for both the EV and PHEV usage cases. This is provided that the deep discharge region (<10% state of charge) of the cell is avoided.

For the performance EV cycle, the thermal model predicts that two edge fin cooling with aluminum fins in unable to limit $\Delta T_{max,cell}$ to below 10 ℃. Without invoking an unpractical fin thickness that is detrimental to the battery volumetric energy density, or using copper fins that is too weighty, fin materials with a higher thermal conductivity and similar or lower density to that of aluminum should be sought for such usage cases.

IX. ACKNOWLEDGEMENTS

The research presented within this paper is supported by the Engineering and Physical Science Research Council through the awards EP/I01585X/1 and EP/M507593/1. The research was undertaken in collaboration with the WMG Centre High Value Manufacturing Catapult (funded by Innovate UK) in collaboration with Aavid Thermacore.

REFERENCES

[1] J. P. Lee, Peater K.;Chung, Youngwoo; OK, Tj;Hwang, KJ;Kim, Jaekyung;Jin, Matt;Park, "Global EV boom – revving up for the next upturn," no. August, 2014.

[2] B. Nykvist and M. Nilsson, "Rapidly falling costs of battery packs for electric vehicles," *Nat. Clim. Chang.*, vol. 5, no. 4, pp. 329–332, Apr. 2015.

[3] A. Dinger, R. Martin, X. Mosquet, M. Rabl, D. Rizoulis, M. Russo, and G. Sticher, "Focus Batteries for Electric Cars," p. 18, 2010.

[4] A. Tourani, P. White, and P. Ivey, "A multi scale multi-dimensional thermo electrochemical modelling of high capacity lithium-ion cells," *J. Power Sources*, vol. 255, pp. 360–367, 2014.

[5] T. M. Bandhauer, S. Garimella, and T. F. Fuller, "A Critical Review of Thermal Issues in Lithium-Ion Batteries," *J. Electrochem. Soc.*, vol. 158, p. R1, 2011.

[6] I. Buchmann, *Batteries in a Portable World*, 3rd ed. Richmond: Cadex Ekectronics Inc., 2011.

[7] D. Doughty and E. P. Roth, "A General Discussion of Li Ion Battery Safety," *Electrochem. Soc. Interface*, pp. 37–44, 2012.

[8] Q. Wang, B. Jiang, B. Li, and Y. Yan, "A critical review of thermal management models and solutions of lithium-ion batteries for the development of pure electric vehicles," *Renew. Sustain. Energy Rev.*, vol. 64, pp. 106–128, 2016.

[9] A. Tourani, P. White, and P. Ivey, "Analysis of electric and thermal behaviour of lithium-ion cells in realistic driving cycles," *J. Power Sources*, vol. 268, pp. 301–314, 2014.

[10] T. Waldmann, M. Wilka, M. Kasper, M. Fleischhammer, and M. Wohlfahrt-Mehrens, "Temperature dependent ageing mechanisms in Lithium-ion batteries – A Post-Mortem study," *J. Power Sources*, vol. 262, pp. 129–135, 2014.

[11] A. Greco, D. Cao, X. Jiang, and H. Yang, "A theoretical and computational study of lithium-ion battery thermal management for electric vehicles using heat pipes," *J. Power Sources*, vol. 257, pp. 344–355, 2014.

[12] I. a. Hunt, Y. Zhao, Y. Patel, and J. Offer, "Surface Cooling Causes Accelerated Degradation Compared to Tab Cooling for Lithium-Ion Pouch Cells," *J. Electrochem. Soc.*, vol. 163, no. 9, pp. A1846–A1852, 2016.

[13] N. Yang, X. Zhang, B. Shang, and G. Li, "Unbalanced discharging and aging due to temperature differences among the cells in a lithium-ion battery pack with parallel combination," *J. Power Sources*, vol. 306, pp. 733–741, 2016.

[14] Y. Ye, L. H. Saw, Y. Shi, and A. a. O. Tay, "Numerical analyses on optimizing a heat pipe thermal management system for lithium-ion batteries during fast charging," *Appl. Therm. Eng.*, vol. 86, pp. 281–291, 2015.

[15] A. Pesaran, "Battery thermal models for hybrid vehicle simulations," *J. Power Sources*, vol. 110, pp. 377–382, 2002.

[16] Z. Rao, S. Wang, M. Wu, Z. Lin, and F. Li, "Experimental investigation on thermal management of electric vehicle battery with heat pipe," *Energy Convers. Manag.*, vol. 65, pp. 92–97, 2013.

[17] L. Fan, J. M. Khodadadi, and a. a. Pesaran, "A parametric study on thermal management of an air-cooled lithium-ion battery module for plug-in hybrid electric vehicles," *J. Power Sources*, vol. 238, pp. 301–312, 2013.

[18] Y. Huo, Z. Rao, X. Liu, and J. Zhao, "Investigation of power battery thermal management by using mini-channel cold plate," *Energy Convers. Manag.*, vol. 89, pp. 387–395, 2015.

[19] Chevrolet, "Cooling fins help keep Chevrolet volt battery at ideal temperature," 2011. [Online]. Available: http://media.gm.com/media/us/en/chevrolet/news.detail.html/content/Pages/news/us/en/2011/Feb/0214_battery.html.

[20] D. Chen, J. Jiang, G. Kim, C. Yang, and A. Pesaran, "Comparison of different cooling methods for lithium ion battery cells," *Appl. Therm. Eng.*, vol. 94, pp. 846–854, 2016.

[21] R. Katkar, Satish; Laurain, Paul; Miccormick, "BATTERY SYSTEM AND METHOD FOR COOLING THE BATTERY SYSTEM - LG CHEM, LTD," 2014.

[22] D. Worwood, Q. Kellner, M. Wojtala, W. D. Widanage, M. Ryan, D. Greenwood, and J. Marco, "A new approach to the internal thermal management of cylindrical battery cells for automotive applications," *J. Power Sources*, vol. 346, pp. 151–166, 2017.

[23] K. Shah, C. McKee, D. Chalise, and a. Jain, "Experimental and numerical investigation of core cooling of Li-ion cells using heat pipes," *Energy*, vol. 113, pp. 852–860, 2016.

[24] R. Zhao, S. Zhang, J. Liu, and J. Gu, "A review of thermal performance improving methods of lithium ion battery: Electrode modification and thermal management system," *J. Power Sources*, vol. 299, pp. 557–577, 2015.

[25] Z. Ling, F. Wang, X. Fang, X. Gao, and Z. Zhang, "A hybrid thermal management system for lithium ion batteries combining phase change materials with forced-air cooling," *Appl. Energy*, vol. 148, pp. 403–409, 2015.

[26] A. a Pesaran, "Battery Thermal Management in EVs and HEVs : Issues and Solutions," *Adv. Automot. Batter. Conf.*, p. 10, 2001.

[27] Chevrolet, "2016 CHEVROLET VOLT BATTERY SYSTEM 2016 CHEVROLET VOLT BATTERY SYSTEM," 2015.

[28] G. Karimi and X. Li, *Thermal management of lithium-ion batteries for electric vehicles*, vol. 37, no. 1. Elsevier Ltd., 2013.

[29] E. Hosseinzadeh, A. Barai, J. Marco, and P. Jennings, "A Comparative Study on Different Cooling Strategies for Lithium-Ion Battery Cells," *Eur. Batter. Hybrid Fuel Cell Electr. Veh. Congr. (EEVC 2017)*, pp. 1–9, 2017.

[30] D. Worwood, R. Algoo, R. McGlen, J. Marco, and D. Greenwood, "A study into different cell-level cooling strategies for cylindrical lithium-ion cells in automotive applications." 3rd International Conference on Powertrain Modelling and Control Testing, Mapping and Calibration, Loughborough, 2016.

[31] D. Worwood, E. Hosseinzadeh, Q. Kellner, J. Marco, D. Greenwood, R. McGlen, W. D. Widanage, A. Barai, and P. Jennings, "Thermal analysis of a lithium-ion pouch cell under aggressive automotive duty cycles with minimal cooling," in *IET Hybrid and Electric Vehicles Conference (HEVC 2016)*, 2016.

[32] G. H. Kim and A. Pesaran, "Battery Thermal Management System Design Modeling," *22nd Int. Batter. Hybrid Fuel Cell Electr. Veh. Conf. Exhib. EVS22*, vol. 1, no. November, pp. 126–133, 2006.

[33] S. Chacko and Y. M. Chung, "Thermal modelling of Li-ion polymer battery for electric vehicle drive cycles," *J. Power Sources*, vol. 213, pp. 296–303, 2012.

[34] U. S. Kim, C. B. Shin, and C. S. Kim, "Effect of electrode configuration on the thermal behavior of a lithium-polymer battery," *J. Power Sources*, vol. 180, pp. 909–916, 2008.